東北大学機関リポジトリ
TOUR
Tohoku University Repository

High Tensile Strength Bulk Glass Alloy Zr65Al10Ni10Cu15 Prepared by Extrusion of Atomiged Glassy Powder

著者	Kato Hidemi, Kawamura Yoshihito, Inoue Akihisa
journal or publication title	Materials transactions, JIM
volume	37
number	1
page range	70-77
year	1996
URL	http://hdl.handle.net/10097/52304

Materials Transactions, JIM, Vol. 37, No. 1 (1996), pp. 70 to 77

High Tensile Strength Bulk Glassy Alloy $Zr_{65}Al_{10}Ni_{10}Cu_{15}$ Prepared by Extrusion of Atomized Glassy Powder

Hidemi Kato†, Yoshihito Kawamura and Akihisa Inoue

Institute for Materials Research, Tohoku University, Sendai 980-77, Japan

This paper deals with the first success of producing a bulk Zr–Al–Ni–Cu glassy alloy with the same mechanical properties as those for the as-cast bulky and melt-spun glassy alloys by extrusion of atomized glassy powder in the supercooled liquid region. A $Zr_{65}Al_{10}Ni_{10}Cu_{15}$ glassy alloy was chosen as the best composition because of the achievement of the lowest viscosity in the supercooled liquid region and an appropriate extrusion temperature (T_e) was evaluated to be about 673 K. The temperature-time-transformation (T.T.T.) diagram in the supercooled liquid region was also determined through the measurement of the time up to crystallization at various temperatures. The bulk glassy alloy prepared by extrusion at an extrusion ratio of 5 and T_e=673 K has a nearly full density above 99% and the T_g, T_x and ΔH_x values are the same as those for the as-atomized glassy powder with a particle size below 150 μm. Furthermore, the extruded bulk alloy also exhibits a tensile strength of 1520 MPa, a Young's modulus of 80 GPa and a tensile fracture strain of 0.02 which are nearly the same as those for the as-cast bulk and melt-spun glassy alloys. The fracture takes place along the maximum shear plane and the fracture surface consists of a well-developed ruggedness similar to the vein pattern typical for amorphous alloys with good bending ductility. The success of producing the bulk glassy alloy with high tensile strength by the extrusion method seems to be encouraging the future development of the Zr-based glassy alloy.

(Received June 7, 1995)

Keywords: *bulk metal glass, zirconium base alloy, extrusion, atomized glassy powder, gas atomization, supercooled liquid region, full density, high tensile strength, shear-type fracture*

I. Introduction

It has recently been reported that bulk glassy alloys in the Ln-, Mg-, Zr- and Ti-based multicomponent systems are produced by various solidification methods such as water quenching[(1)(2)], arc melting[(3)], copper mold casting[(4)–(6)], high-pressure die casting[(7)(8)] and unidirectional solidification[(9)]. Although these solidification methods are very attractive for the direct production of bulk glassy alloys, they can be applied only to the glassy alloys with large glass-forming ability and the maximum sample thickness has also been limited to less than about 25 mm[(10)]. In addition to these solidification methods, a consolidation method by utilizing high viscous flow in the supercooled liquid region is known as an alternative method to form a bulk glassy alloy. This method has an advantage leading to the elimination of the limitation of maximum sample thickness. However, it is very difficult to obtain a truely bonding state among glassy particles in a glassy state without generation of any crystalline phase. The difficulty can be understood from a number of previous data[(11)] where the bulk amorphous alloys prepared by extrusion of atomized amorphous powders exhibit tensile strength much lower than those for the corresponding melt-spun amorphous ribbons. No successful result in which the tensile strength of the extruded bulk amorphous alloy is nearly the same as that for the corresponding melt-spun amorphous ribbon has been obtained in spite of a number of reports on the preparation and mechanical properties of consolidated bulk amorphous alloys. The much lower tensile strength resulting from the lack of the truely bonding state is presumably because the supercooled liquid region is too narrow to achieve high viscous flow. More recently, we have found that the Ln-[(12)(13)], Mg-[(14)(15)], Zr-[(16)(17)] and Ti-[(18)(19)] based glassy alloys have a wide supercooled liquid region before crystallization and the largest value of the supercooled liquid region defined by the difference between glass transition temperature (T_g) and crystallization temperature (T_x), $\Delta T_x(=T_x-T_g)$ reaches 127 K[(20)]. When the atomized powders of the new glassy alloys with ΔT_x above 100 K are used as raw materials for extrusion, it is expected that the powders in the extruded bulk glassy alloy have a truely bonding state and the bulk alloy exhibits the same high tensile strength as that for the corresponding melt-spun glassy ribbon. This paper is intended to search an appropriate extrusion condition for the preparation of bulk glassy Zr–Al–Ni–Cu alloys and to examine the structure and mechanical properties of the extruded bulk glassy alloys.

II. Experimental Procedure

Alloys with composition $Zr_{60}Al_{10}Ni_xCu_{30-x}$ and $Zr_{65}Al_{10}Ni_xCu_{25-x}$ (x=5, 10, 15 and 20 at%) were prepared by arc melting pure metals of Zr, Al, Ni and Cu in an argon atmosphere. The prealloyed ingot was remelted at 1473 K in an argon atmosphere and atomized into spherical powder at a dynamic pressure of 9.8 MPa by high-pressure He gas atomization. The particle size fraction of the atomized powders was measured by the laser

† Graduate Student, Tohoku University.

trap method. The powder was sieved with meshes and then precompacted up to a density of about 65% into a steel can. The sequent process of atomization, sieving and precompaction was made in a well-controlled atmosphere with oxygen and moisture concentrations below 0.5 ppm. Subsequently, the precompacted powder was degassed for 900 s at 473 K and then sealed by welding. The powders sealed in the copper can were extruded at various extrusion temperatures between 673 and 713 K and different extrusion ratios ranging from 3 to 5. The extrusion ratios were chosen because the minimum extrusion ratio leading to full density (≡100%) was about 2.5[21]. The structures of as-atomized powder and extruded bulk alloy were examined by X-ray diffractometry, optical microscopy (OM) and transmission electron microscopy (TEM) and their thermal stability was examined by differential scanning calorimetry (DSC). The OM sample was etched for 10 s at 298 K in a solution of 1% hydrofluoric acid and 99% distilled water and the TEM thin foils were prepared by mechanical cutting of the extruded alloy, followed by electrical polishing at approximately 210 K in a solution of 10% nitric acid and 90% methanol in volume. The tensile testing or the extruded bulk alloy was made at a strain rate of $5.0 \times 10^{-4}\,s^{-1}$ at room temperature. The tensile fracture surface appearance was examined by scanning electron microscopy (SEM).

With the aim of producing efficiently an extruded bulk alloy with good mechanical properties, preliminary researches on the onset temperature for thermal embrittlement, the temperature dependence of viscosity and the temperature-time-transformation (T.T.T.) relation were performed for melt-spun Zr-Al-Ni-Cu glassy ribbons with a thickness of about 30 μm. The thermal embrittlement was evaluated by a simple bending test for the samples annealed for 60 s at various temperatures. The temperature dependence of viscosity was measured by thermal mechanical analyses. The T.T.T. diagram was determined by measuring the time up to the onset of an exothermic reaction due to crystallization in the DSC curve during isothermal annealing for the samples heated up to various temperatures at a rate of 0.67 K/s.

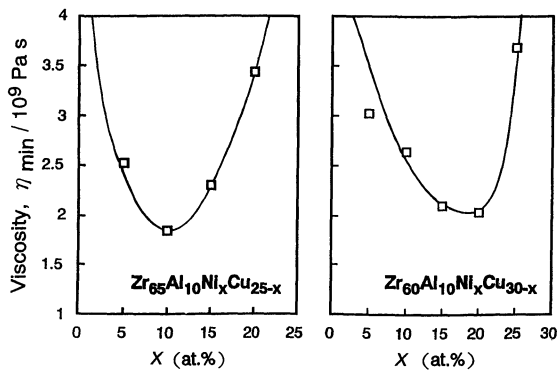

Fig. 1 Change in the minimum viscosity (η_{min}) with Ni content for glassy $Zr_{65}Al_{10}Ni_xCu_{25-x}$ and $Zr_{60}Al_{10}Ni_xCu_{30-x}$ alloys.

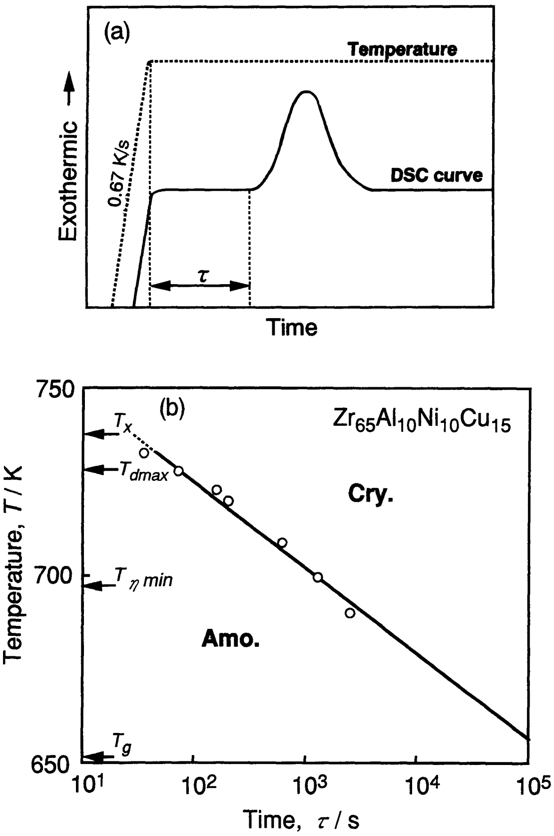

Fig. 2 (a) A method to measure the annealing time (τ) up to the start of crystallization, and (b) T.T.T. diagram for a glassy $Zr_{65}Al_{10}Ni_{10}Cu_{15}$ alloy. The data of the onset temperature of crystallization (T_x), the ductile-brittle transition temperature ($T_{d_{max}}$), the temperature at which the viscosity is minimum ($T_{\eta_{min}}$) and the glass transition temperature (T_g) are also shown for comparison.

III. Results

Figure 1 shows the compositional dependence of the minimum viscosity in the supercooled liquid for the glassy $Zr_{65}Al_{10}Ni_xCu_{25-x}$ and $Zr_{60}Al_{10}Ni_xCu_{30-x}$ alloys. The viscosity shows the lowest value of 1.85×10^9 Pa·s for the $Zr_{65}Al_{10}Ni_{10}Cu_{15}$ alloy, indicating the possibility that the alloy exhibits the largest viscous flow in the supercooled liquid because of the widest supercooled liquid region. Figure 2 shows the T.T.T. diagram and the maximum temperature for the ductile-brittle transition ($T_{d_{max}}$) for the glassy $Zr_{65}Al_{10}Ni_{10}Cu_{15}$ alloy having the lowest viscosity. As shown in Fig. 2, the annealing time (τ) up to the onset of crystallization at the temperature ($T_{\eta_{min}}$=696 K) where the minimum viscosity of 1.85×10^9 Pa·s is obtained is measured to be 1700 s. This result indicates the possibility that the extrusion within a short time below 1700 s at $T_{\eta_{min}}$=696 K causes the formation of a bulk $Zr_{65}Al_{10}Ni_{10}Cu_{15}$ glass with good ductility.

Figure 3 shows the surface morphology of the as-atomized $Zr_{65}Al_{10}Ni_{10}Cu_{15}$ glassy powder with a particle size fraction smaller than 75 μm. No appreciable contrast revealing the formation of a crystalline phase is seen on the outer surface of any particles. The average particle size in the present atomization condition was measured

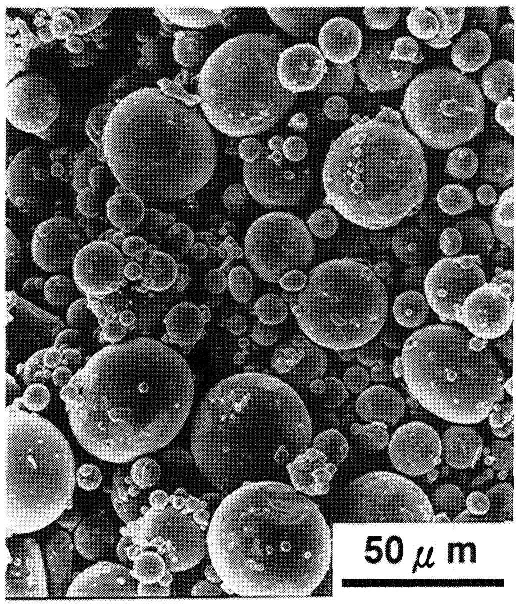

Fig. 3 Outer surface appearance of as-atomized $Zr_{65}Al_{10}Ni_{10}Cu_{15}$ glassy powder.

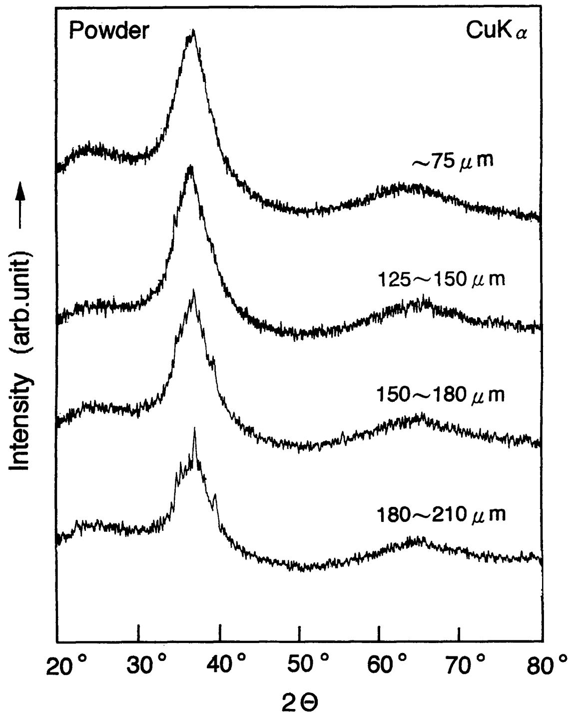

Fig. 4 X-ray diffraction patterns of as-atomized $Zr_{65}Al_{10}Ni_{10}Cu_{15}$ powder with particle size fractions of <75 μm, 125-150 μm, 150-180 μm and 180-210 μm.

to be about 75 μm. In order to confirm the formation of a glassy single phase without any crystallinity, the X-ray diffraction patterns taken from the powders with different particle size fractions are shown in Fig. 4. The patterns show clearly that a glassy phase without crystallinity is formed in the particle size fraction of 125 to 150 μm and the further increase in the particle size fraction

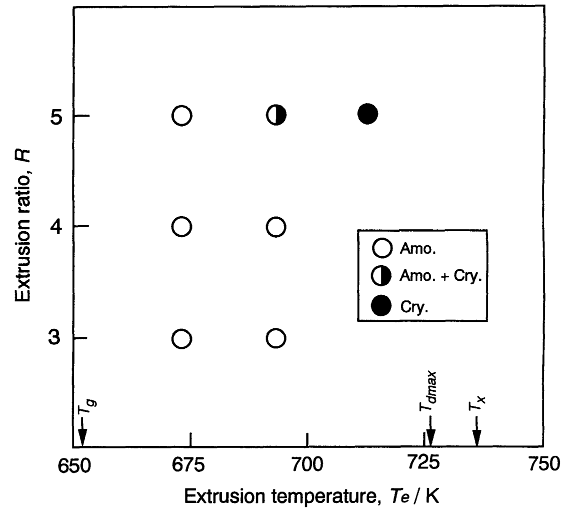

Fig. 5 Change in the structure of an as-extruded $Zr_{65}Al_{10}Ni_{10}Cu_{15}$ alloy with extrusion ratio (R) and extrusion temperature (T_e).

causes the coexistence of a small amount of crystalline phase into the glassy phase. Consequently, the subsequent extrusion was made for the glassy powders with a particle size fraction below 150 μm.

Figure 5 shows the relation among the extrusion ratio (R), the extrusion temperature (T_e) and the structure of the extruded bulk for the $Zr_{65}Al_{10}Ni_{10}Cu_{15}$ glassy powder, together with the data of T_g, $T_{d_{max}}$ and T_x. A glassy phase is maintained in the extrusion condition where T_e is below 693 K for $R=3$ and 4 and below 673 K for $R=5$ and the further increase in T_e causes the coexistence of a crystalline phase. As examples, Fig. 6 shows bright-field electron micrographs and selected-area electron diffraction patterns of the bulk alloys extruded at $T_e=673$ K, $R=5$ (a), $T_e=693$ K, $R=5$ (b) and $T_e=693$ K, $R=4$ (c). It is seen that the extruded bulk alloys consist of a glassy single phase at the conditions (a) and (c) and glassy and crystalline phases at the condition (b). Furthermore, the optical micrographs of the bulk alloy obtained at $R=5$ and $T_e=673$ K shown in Fig. 7 reveal that neither appreciable void nor intergranular boundary is seen in the cross sectional structure of the extruded bulk alloy which keeps the glassy phase. The feature of the DSC curves and the heat of crystallization for the bulk alloys at $T_e=673$ K and $R=3$, 4 and 5 are the same as those for the as-atomized powder, as shown in Fig. 8. The structural and thermal data indicate clearly that the extruded bulk alloys have a full density caused by a truely bonding state and keep nearly the same glassy structure as that for the as-atomized glassy powder.

Tensile testing specimens with the gauge dimensions of 8.4 mm in length and 3.0×1.5 mm^2 in cross section were made from the bulk glassy alloy extruded at the condition of $T_e=673$ K and $R=5$ and the morphology of the specimen is shown in Fig. 9. Figure 9 also shows the tensile stress-strain curve of the specimen at room temperature, together with the data of the bulk glassy alloy prepared by a metallic mold casting method. No distinct

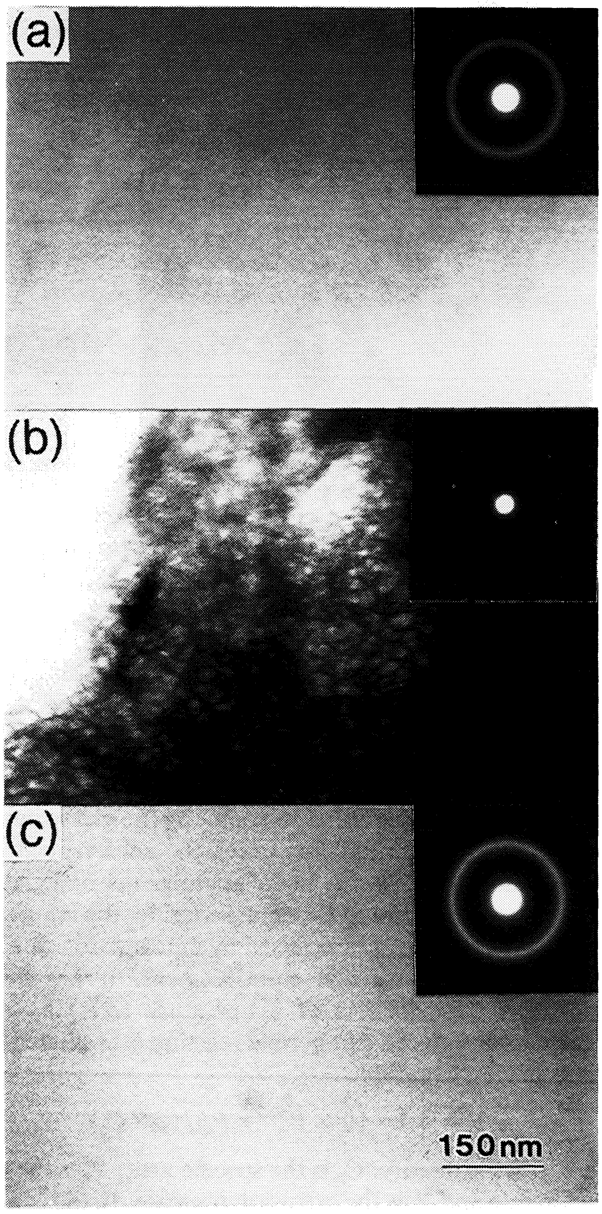

Fig. 6 Bright-field electron micrographs and selected-area electron diffraction patterns of the $Zr_{65}Al_{10}Ni_{10}Cu_{15}$ alloys extruded in different conditions. (a) $R=5$, $T_e=673$ K, (b) $R=5$, $T_e=693$ K, and (c) $R=4$, $T_e=693$ K.

difference in the feature of the stress-strain curve is seen between the extruded alloy and the cast bulk glassy alloy. One can see clearly that the extruded bulk alloy has nearly the same high tensile strength as that for the cast bulk glassy alloy. Table 1 also summarizes σ_f, E and ε_f of the extruded bulk alloys obtained at different extrusion ratios and extrusion temperatures, together with the data of structure and relative density. The extruded glassy alloys exhibit a high tensile strength (σ_f) of 1520 MPa, a Young's modulus (E) of 80 GPa and a fracture strain (ε_f) of 0.02. It is confirmed that the σ_f, E and ε_f values are nearly the same as those ($\sigma_f \equiv 1570$ MPa, $E \equiv 80$ GPa and $\varepsilon_f \equiv 0.02$)[21] for the cast bulk glassy alloy with a thickness of 1.5 mm and the melt-spun glassy ribbon with a thickness of 30 μm. However, the σ_f and ε_f values decrease slightly with decreasing R and significantly by the coexistence of the crystalline phase. At any event, the achievement of the extruded bulk glassy alloy with the same σ_f and ε_f as those for the cast bulk glassy alloy and melt-spun glassy ribbon is believed to be the first evidence. The tensile fracture of the extruded alloy takes place along the maximum shear plane which is declined by about 45 degrees to the direction of tensile load, as shown in Fig. 10. Furthermore, the scanning electron micrograph shown in Fig. 11 reveals that the tensile fracture surface contains a significant ruggedness similar to the vein pattern in almost all the region and no shell-like pattern typical for a brittle amorphous alloy is seen. The feature of the tensile fracture surface appearance is also the same as that for the cast bulk and melt-spun glassy alloys, indicating that the present extruded glassy alloy also has good ductility.

IV. Discussion

It is shown in Section III that the extruded bulk alloy exhibits the high tensile strength and the tensile fracture mode which are nearly the same as those for the cast bulk and melt-spun glassy alloys. Here, it is important to investigate the reason for the achievement of the high tensile strength for the present extruded bulk alloy. The high tensile strength is thought to be due to the combination of the achievement of a truely bonding state among the glassy particles without appreciable voids and the maintenance of a glassy structure with good ductility. No appreciable contrast revealing the absence of the truely bonding state among the particles is seen in the optical micrographs taken from the transverse and longitudinal cross sections of the extruded alloy. Furthermore, we cannot see any contrast revealing the existence of a crystal-

Table 1 Structure, relative density and mechanical properties of the bulk $Zr_{65}Al_{10}Ni_{10}Cu_{15}$ alloys extruded at various conditions. The data of the cast bulk sheet and melt-spun ribbon are also shown for comparison.

Specimen	Extrusion condition R	T_e(K)	Structure	Tensile strength σ_f(MPa)	Young's modulus E(GPa)	Fracture strain ε_f	Relative density D(%)
	5	693	Amo.+Cry.	930	117	0.009	99.9
Extruded bulk	5	673	Amo.	1520	80	0.020	99.4
(d=10~12 mmϕ)	4	693	Amo.	1420	78	0.019	99.5
	3	673	Amo.	1420	78	0.019	99.1
Cast sheet (t=1.5 mm)			Amo.	1570	80	0.020	99.9
Melt-spun ribbon (t=30 μm)			Amo.	1440	—	—	100

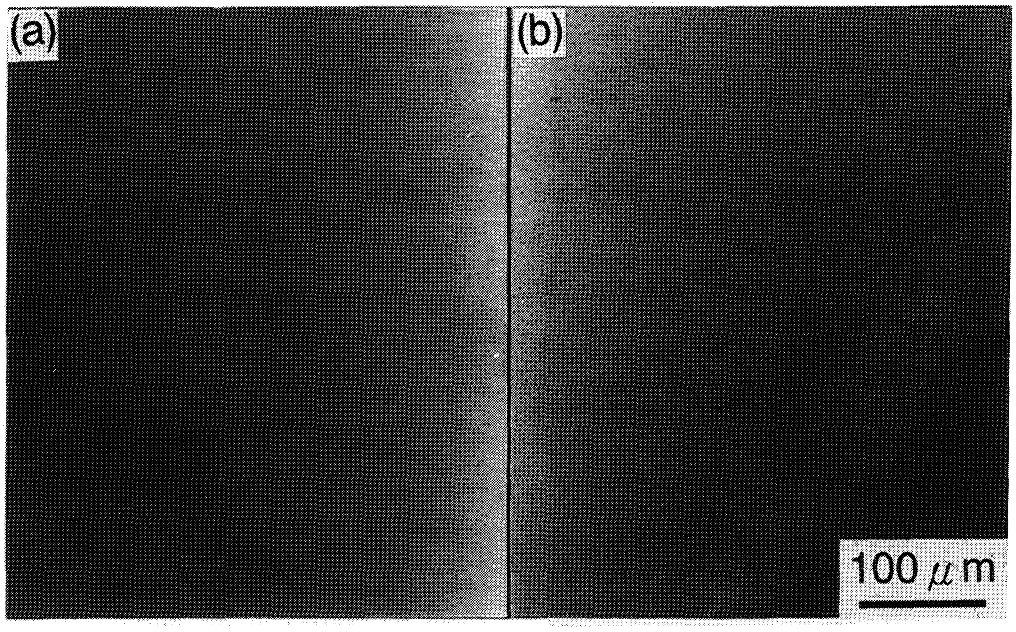

Fig. 7 Optical micrographs of the cross sectional structure of the extruded $Zr_{65}Al_{10}Ni_{10}Cu_{15}$ glassy alloy obtained by $R=5$ and $T_e=673$ K. (a) transverse cross section, (b) longitudinal cross section.

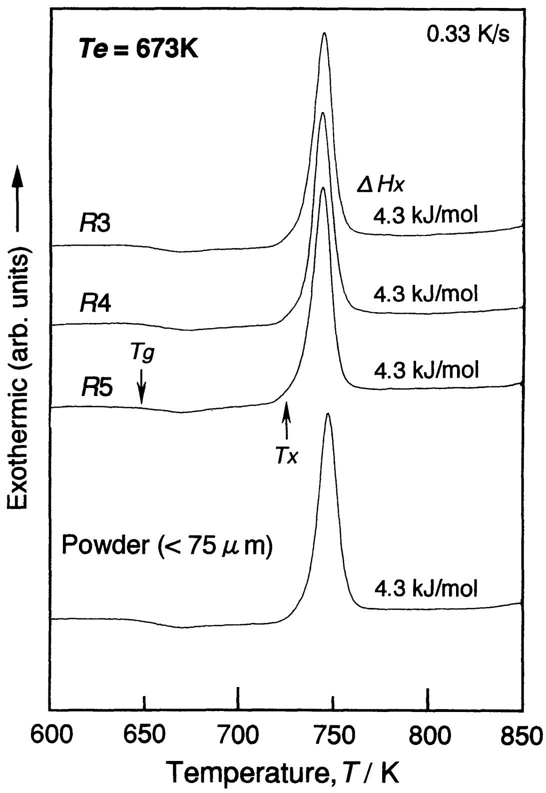

Fig. 8 DSC curves of the extruded $Zr_{65}Al_{10}Ni_{10}Cu_{15}$ alloy obtained at $T_e=673$ K and $R=3$, 4 and 5. The data of the atomized powder with a particle size fraction smaller than 75 μm are also shown for comparison.

line phase and the relative density is measured to be as high as about 99%. These results allow us to conclude that the extruded bulk alloy consists of a glassy single phase with a truely bonding state among the glassy particles. Another important factor for the achievement of high tensile strength is due to the maintenance of a glassy state with good ductility. One must consider the influence of the rise of temperature caused by deformation during extrusion on the thermal embrittlement. It has been reported[22] that the rise of temperature (ΔT_e) by the deformation-induced exothermic reaction is evaluated by the following equation.

$$\Delta T_e=(1.1\times 10^4\times V_e^{0.64}\times P_e)/(\rho\times C_p)$$

Here, ρ is the density, C_p is the specific heat, V_e is the extrusion rate and P_e is the extrusion pressure. In the condition where the ρ, C_p, V_e and P_e are 6.70 Mg/m^3, 30 J/mol·K^{-1}, 1 mm/s and 1 GPa, respectively, for the $Zr_{65}Al_{10}Ni_{10}Cu_{15}$ alloy, the ΔT_e value is estimated to be 55 K. In order to avoid the embrittlement casued by the rise of temperature during extrusion, the extrusion temperature should be reduced by 55 K than the maximum temperature ($T_{d_{max}}$) of ductile to brittle transition by annealing for 60 s in the present glassy alloy. Since the $T_{d_{max}}$ is measured to be 728 K as shown in Fig. 2, the maximum extrusion temperature which can avoid the embrittlement resulting from the rise of temperature during extrusion is determined to be 673 K. This evaluation is consistent with the present result that the bulk alloy extruded at 673 K exhibits the high tensile strength and good ductility comparable to those for the cast bulk and melt-spun glassy alloys.

It is also known that the ductility of an amorphous alloy is strongly dependent on the degree of structural relaxation. That is, there is a tendency for ductility to decrease with proceeding structural relaxation. Figures 12 and 13 show the structural relaxation behavior upon continuous

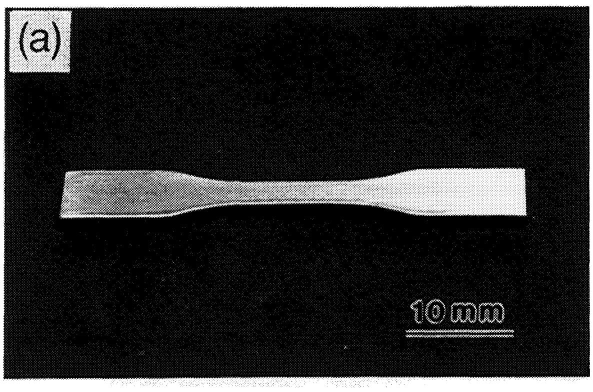

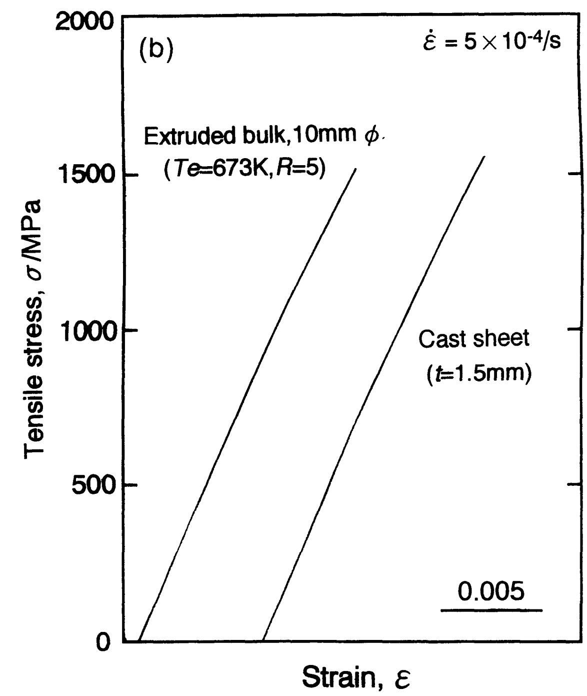

Fig. 9 (a) Morphology of the glassy $Zr_{65}Al_{10}Ni_{10}Cu_{15}$ specimen used for tensile testing. The specimen was made from the bulk glassy alloy obtained by extrusion at $T_e=673$ K and $R=5$ by mechanical cutting. (b) Tensile stress-strain curve of the specimen. The data on the cast bulk glassy sample are also shown for comparison.

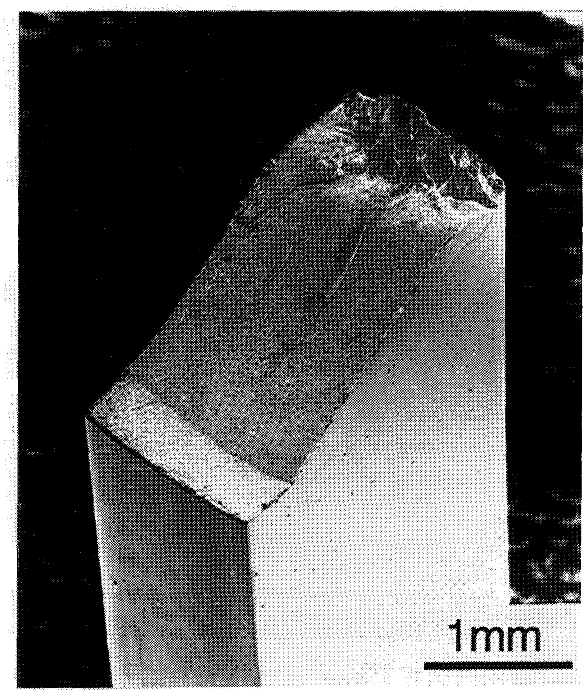

Fig. 10 Tensile fracture appearance of the extruded $Zr_{65}Al_{10}Ni_{10}Cu_{15}$ glassy alloy.

heating for the as-atomized glassy powder with a particle size below 75 μm and glassy bulk extruded at $T_e=673$ K and $R=5$, respectively, for the $Zr_{65}Al_{10}Ni_{10}Cu_{15}$ alloy. Although the difference between $C_{p,q}$ and $C_{p,s}$ is significant for the powder, the $C_{p,q}$ of the extruded bulk alloy approaches to the $C_{p,s}$ curve. The difference in C_p between the sample heated once for 60 s at 710 K ($C_{p,s}$) and the as-prepared samples ($C_{p,q}$), $\Delta C_p(=C_{p,q}-C_{p,s})$, is due to the structural relaxation caused by continuous heating. From the data of the ΔC_p as a function of temperature for the powder, the extruded bulk and the melt-spun glassy ribbon with a thickness of 30 μm shown in Fig. 14, the onset temperature of structural relaxation (T_r) is measured to be about 395 K for the melt-spun ribbon, 400 K for the as-atomized powder and 545 K for the extruded alloy. Furthermore, the heat of structural relaxation (ΔH_r) evaluated by $\int \Delta C_p(=C_{p,s}-C_{p,q})\mathrm{d}T$, $\Delta C_p>0$, is 1590 J/mol for the ribbon, 1340 J/mol for the powder and 250 J/mol for the extruded bulk. The T_r and ΔH_r values indicate clearly that the degree of unrelaxed glassy structure is greater in the order of the melt-spun ribbon > as-atomized powder ≫ extruded bulk. Here, it is to be noticed that the extruded bulk sample still keeps an unrelaxed atomic configuration, though the extrusion was made at the high temperature of 673 K above T_g. Since the heating for 900 s at 673 K causes the complete disappearance of the heat of structural relaxation, the heat of structural relaxation of 250 J/mol seems to be introduced by the extrusion treatment at 673 K and the subsequent cooling to room temperature. The extrusion-induced unrelaxed atomic configuration is thought to be the reason for the maintenance of the good ductility which enables the achievement of nearly the same high tensile strength as those for the as-cast and melt-spun glassy alloys. This concept is consistent with the present result (Table 1) that the tensile strength for the extruded glassy alloys obtained at the same extrusion temperature increases with increasing extrusion ratio. The effectiveness of the deformation at the high temperature near T_g for the maintenance of good ductility has also been recognized for the Fe- and Co-based amorphous alloy wires[23] and Ln–Al–Ni glassy alloys[24].

V. Summary

The possibility that a bulk glassy alloy with high tensile strength and good ductility is prepared by extrusion of atomized glassy powder has been examined for Zr–Al–Ni–Cu glassy alloys exhibiting a wide supercooled liquid

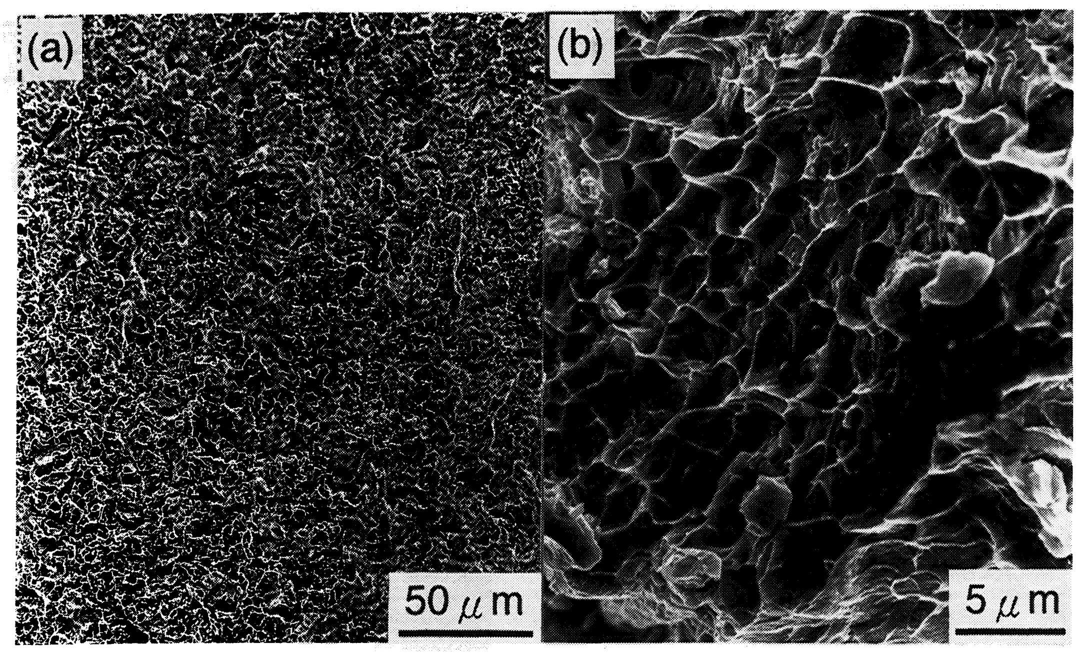

Fig. 11 Tensile fracture surface appearance of the extruded $Zr_{65}Al_{10}Ni_{10}Cu_{15}$ glassy alloy.

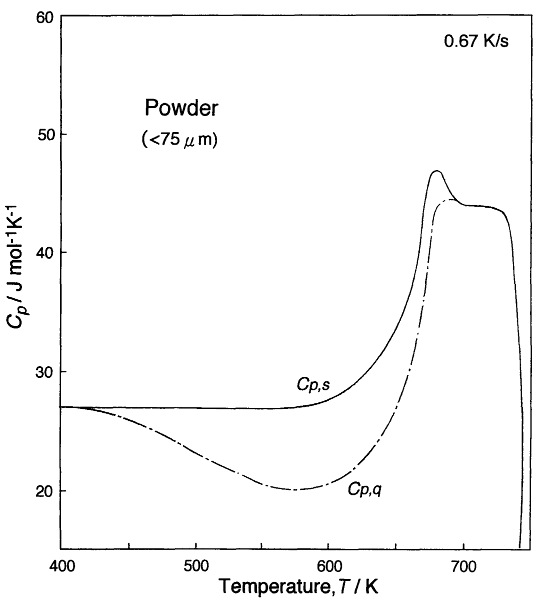

Fig. 12 Thermogram ($C_{p,q}$) of the as-atomized glassy $Zr_{65}Al_{10}Ni_{10}Cu_{15}$ powder. The $C_{p,s}$ represents the data of the powder heated once to 710 K fo 60 s.

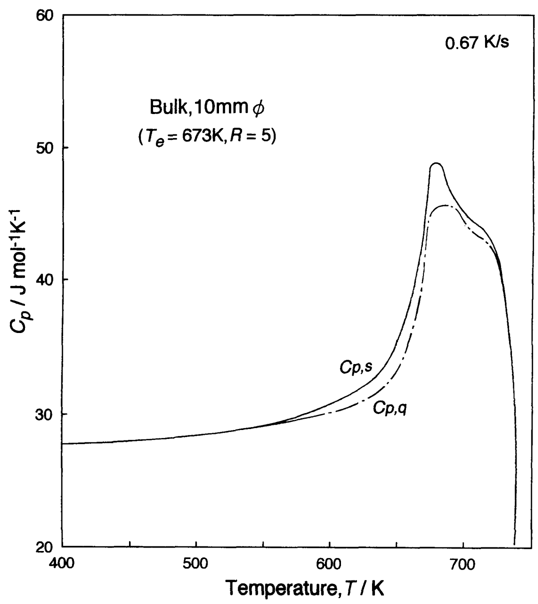

Fig. 13 Thermogram ($C_{p,q}$) of the extruded glassy $Zr_{65}Al_{10}Ni_{10}Cu_{15}$ bulk. The $C_{p,s}$ represents the data of the bulk heated once to 710 K for 60 s.

region before crystallization. The results obtained are summarized as follows.

(1) The smallest viscosity in the supercooled liquid region before crystallization was 1.85×10^9 Pa·s at 696 K for a $Zr_{65}Al_{10}Ni_{10}Cu_{15}$ glassy alloy with the widest supercooled liquid region. Consequently, the Zr–Al–Ni–Cu alloy was chosen for the subsequent extrusion.

(2) The T.T.T. diagram was determined for the $Zr_{65}Al_{10}Ni_{10}Cu_{15}$ glassy alloy and the maximum temperature at which the sample becomes brittle after annealing for 60 s was determined to be 728 K.

(3) The bulk alloys extruded at the conditions of 3 to 5 for R and 673 to 693 K for T_e have a relative density of about 99% and the thermal propeties of T_g, T_x, ΔT_x and ΔH_x are the same as those for the as-atomized powder with a particle size fraction below 150 μm.

(4) The bulk glassy alloy extruded at $R=5$ and $T_e=673$ K exhibits a tensile strength of 1520 MPa which is nearly the same as those (1440 to 1570 MPa) for the as-cast bulk and the melt-spun glassy alloys. No appreciable difference in Young's modulus and tensile fracture strain is also seen between the extruded bulk and the cast or

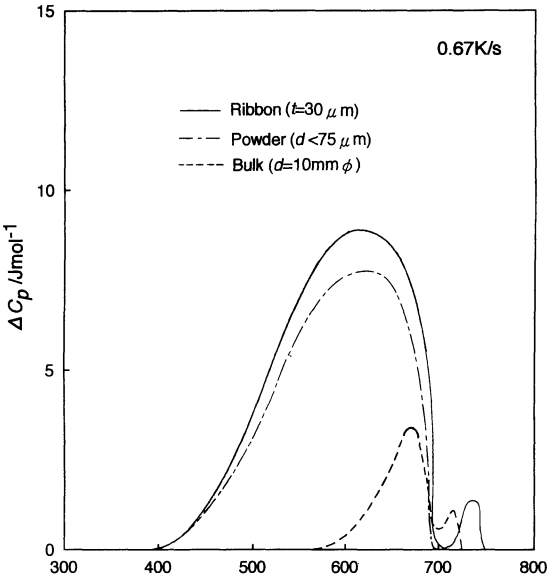

Fig. 14 Temperature dependence of the difference in specific heat between $C_{p,q}$ and $C_{p,s}$, $\Delta C_p(=C_{p,q}-C_{p,s})$ for the $Zr_{65}Al_{10}Ni_{10}Cu_{15}$ glassy alloy in the as-atomized powder, extruded bulk and melt-spun ribbon forms.

melt-spun glassy alloys.

(5) The tensile fracture takes place in the shear type mode and the fracture surface consists of a well-developed dimple pattern which is similar to the vein pattern typical for the melt-spun glassy alloy with good bending ductility. The present success of producing the bulk glassy alloys with the same mechanical properties as those for the corresponding melt-spun glassy ribbon by utilizing the viscous flow in the supercooled liquid region seems to affect greatly the future development of bulk glassy alloys.

Acknowledgment

The author (A. Inoue) is grateful to the Grant-in-Aid for Specially Promoted Research of The Ministry of Education, Science and Culture for support of this research.

REFERENCES

(1) A. Inoue, K. Kita, T. Zhang and T. Masumoto: Mater. Trans., JIM, **30** (1989), 722.
(2) A. Inoue, T. Zhang, N. Nishiyama, K. Ohba and T. Masumoto: Mater. Trans., JIM, **34** (1993), 1234.
(3) A. Inoue and T. Zhang: Metals, No. 3, (1994), p. 47.
(4) A. Inoue, A. Kato, T. Zhang, S. G. Kim and T. Masumoto: Mater. Trans., JIM, **32** (1991), 609.
(5) A. Inoue, T. Saito, H. Yamamoto: J. Mater. Sci. Lett., **12** (1993), 946.
(6) A. Inoue, T. Zhang and T. Masumoto: Mater. Trans., JIM, **36** (1995), 391.
(7) A. Inoue, T. Nakamura, N. Nishiyama and T. Masumoto: Mater. Trans., JIM, **33** (1992), 937.
(8) A. Inoue, T. Nakamura, T. Sugita, T. Zhang and T. Masumoto: Mater. Trans., JIM, **34** (1993), 351.
(9) A. Inoue Y. Yokoyama, Y. Shinohara and T. Masumoto: Mater. Trans., JIM, **35** (1994), 923.
(10) A. Inoue: Mater. Trans., JIM, **36** (1995), 866.
(11) R. B. Schwarz: *Rapidly Solidified Alloys*, ed. by H. H. Liebermann, Marcel Dekker, New York, (1993), p. 157.
(12) A. Inoue, T. Zhang and T. Masumoto: Mater. Trans., JIM, **30** (1989), 965.
(13) A. Inoue, H. Yamaguchi, T. Zhang and T. Masumoto: Mater. Trans., JIM, **31** (1990), 104.
(14) A. Inoue, K. Ohtera, K. Kita and T. Masumoto: Jpn. J. Appl. Phys., **27** (1988), L2248.
(15) A. Inoue, K. Kohinata, K. Ohtera, A. P. Tsai and T. Masumoto: Mater. Trans., JIM, **30** (1989), 378.
(16) A. Inoue, T. Zhang and T. Masumoto: Mater. Trans., JIM, **31** (1990), 177.
(17) A. Inoue, T. Zhang and T. Masumoto: J. Non-Cryst. Solids, **156–158** (1993), 473.
(18) A. Inoue, N. Nishiyama, K. Amiya, T. Zhang and T. Masumoto: Mater. Lett., **19** (1994), 131.
(19) A. Peker and W. L. Johnson: Appl. Phys. Lett., **63** (1993), 2342.
(20) T. Zhang, A. Inoue and T. Masumoto: Mater. Trans., JIM, **32** (1991), 1005.
(21) A. Inoue, T. Zhang and T. Masumoto: Mater. Trans., JIM, **36** (1995), 391.
(22) Y. Kawamura, A. Inoue, K. Sasamori and T. Masumoto: Mater. Sci. Eng., **A181/A182** (1994), 1174.
(23) A. Inoue, N. Yano, H. S. Chen, M. Hagiwara and T. Masumoto: Mater. Sci. Eng., **77** (1986), 45.
(24) A. Inoue, T. Zhang and T. Masumoto: J. Non-Cryst. Solids, **156–158** (1993), 547.